CrossMark

RESEARCH PAPER

A way of estimating the characteristic slip displacement

Jeen-Hwa Wang

Abstract During the ruptures of an earthquake, the strain energy, ΔE, will be transferred into, at least, three parts, i.e., the seismic radiation energy (E_s), fracture energy (E_g), and frictional energy (E_f), that is, $\Delta E = E_s + E_g + E_f$. Friction, which is represented by a velocity- and state-dependent friction law by some researchers, controls the three parts. One of the main parameters of the law is the characteristic slip displacement, D_c. It is significant and necessary to evaluate the reliable value of D_c from observed and inverted seismic data. Since D_c controls the radiation efficiency, $\eta_R = E_s / (E_s + E_g)$, the value of η_R is a good constraint of estimating D_c. Integrating observed data and inverted results of source parameters from recorded seismograms, the values of E_s and E_g of an earthquake can be measured, thus leading to the value of η_R. The constraint used to estimate the reliable value of D_c will be described in this work. An example of estimates of D_c based on the observed and inverted values of source parameters of the September 20, 1999 M_S 7.6 Chi-Chi (Ji-Ji), Taiwan region, earthquake will be presented.

Keywords Characteristic slip displacement · Seismic radiation energy · Fracture energy · Radiation efficiency

1 Introduction

Friction controls the earthquake rupture processes. Experimental and theoretical studies showed two effects affecting the friction strength: the direct effect and the evolution one (Dieterich 1978, 1979; Rice 1983; Ruina 1983; Beeler et al. 1994; Marone 1998). The direct effect shows an instantaneous change of friction strength with a change in velocity, while the evolution effect evolves with slip following a change in velocity. Unstable slip in rock can result only when the evolution effect is larger than the direct one, which leads to the so-called velocity-weakening process. Bizzarri (2011) made a comprehensive description and review about the constitution laws and their intrinsic properties of friction, including time-weakening law, position-weakening law, slip-dependent law, rate-dependent law, and rate- and state-dependent law. This study, focus on the estimate of the characteristic slip displacement, D_c, of rate- and state-dependent law. D_c is denoted by L and named the slip-weakening distance by Bizzarri (2011), Ulutaş (2008, 2013, 2015), and Ulutaş et al. (2006, 2011). One of the weak points is that, as shown below, the law cannot be defined when the velocity is zero.

The one-state-variable slip and slowness (or aging) laws proposed by Dieterich (1978, 1979) and Ruina (1983) have been long used to represent the state-dependent evolution effect. Some authors compared the two laws based on the quasi-static model, which was often regarded as an acceptable approximation of the dynamic model (e.g., Rice and Ruina 1983; Gu et al. 1984; Rice and Tse 1986), especially for low velocities. From numerical simulations of earthquake nucleation on faults, Dieterich (1992) stressed that in most cases, the results using the two laws are similar. Rice and Ben-Zion (1996) stated that the slip law leads to periodically repeated events, but the slowness one allows apparently chaotic sequences of large events. Roy and Marone (1996) stated that pre-seismic slip is larger for the slowness law than for the slip law.

Ruina (1983) defined the rate- and state-dependent friction strength, μ, which employs state variables, θ, in the

J.-H. Wang (✉)
Institute of Earth Sciences, Academia Sinica,
P.O. Box 1-55, Nangang, Taipei 115, Taiwan
e-mail: jhwang@earth.sinica.edu.tw

following form: $\mu = \mu_0 + a\ln(v/v_0) + b\ln(\theta v_0/D_c)$, where a and b are two constants, v is the sliding velocity, v_0 is the reference velocity, and D_c is the characteristic slip distance. This expression leads to $\mu = \mu_0$ when $v = v_0$ and $\theta = D_c/v_0$. It is noted that the system is not at rest when $v = v_0$. The value of v_0 is usually considered to be a constant and not regarded as a significant parameter controlling the dynamic friction strength. Contributions to the total friction strength are scaled by a for the direct effect and b for the evolution effect. The three parameters a, b, and D_c for some rocks were determined experimentally (e.g., Dieterich 1979; Reinen and Weeks 1993), and the experimental values vary in large ranges.

Two one-state-variable friction laws are commonly used to describe the state-dependent evolution effect. One is the slip law given by $d\theta/dt = -(\theta v/D_c)\ln(\theta v/D_c)$. When $v = 0$, $d\theta/dt$ approximates to zero using the l'Hospital's theorem. This implicates that no evolution occurs at zero sliding velocity. The other is slowness law given by $d\theta/dt = 1 - \theta v/D_c$. This equation shows that state is proportional to slowness, i.e., $\theta = D_c/v$ when $d\theta/dt = 0$. A detailed description can be found elsewhere (Dieterich 1979; Ruina 1983; Marone 1998; Wang 2009a).

After an earthquake rupture, the frictional stress on a fault plane decreases from an initial level, σ_0, to a dynamical one, σ_d, which is equal to or smaller than the final one, σ_f (cf. Kanamori and Heaton 2000; Kanamori and Brodsky 2004). The process can be seen in Fig. 1. The static stress drop and the dynamic stress drop are, respectively, $\Delta\sigma_s = \sigma_0 - \sigma_f$ and $\Delta\sigma_d = \sigma_0 - \sigma_d$. The friction law is complicated and depends upon either the slip or slip rate (cf. Marone 1998; Wang 2002). The friction law is displayed by a dashed line as shown in Fig. 1 and can be approximated by a piece-wise linear function. The strain energy, ΔE, can be transferred into, at least, three parts, i.e., the seismic radiation energy (E_s), the fracture energy (E_g), and the frictional energy (E_f),
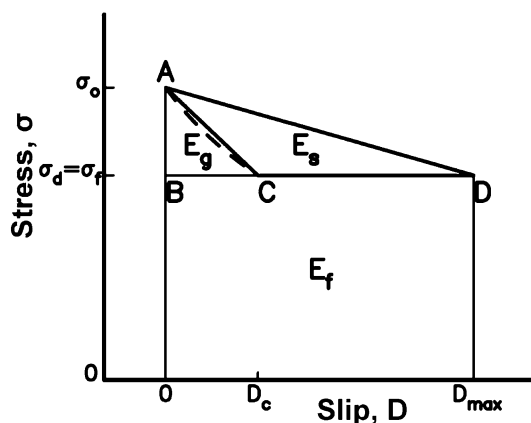

Fig. 1 The stress-slip function. The *symbols* are explained in the text (after Wang 2006a)

that is, $\Delta E = E_s + E_g + E_f$. According to the rate- and slip-weakening friction law, small E_g is associated with a short characteristic slip displacement, D_c. Venkataraman and Kanamori (2004) defined the radiation efficiency, η_R, to be the ratio of E_s to $(E_s + E_g)$, i.e., $\eta_R = E_s/(E_s + E_g)$. D_c related to η_R, which is a function of the ratio of rupture velocity over the S-wave velocity.

The D_c is the characteristic slip displacement, within which the frictional stress changes from a static one to a steady dynamic one (cf. Marone 1998; Wang 2002, 2009a). Laboratory results show D_c to be 10^{-5}–10^{-3} m (Marone 1998). On the other hand, for real earthquakes, Mikumo et al. (2003) obtained D_c of 0.1 m to few meters. Their approach is based on the estimate of characteristic slip displacement at each point on the fault as the slip (D'_c) at the time of peak slip velocity, supposing that the traction reaches its minimum value in that time. Fukuyama et al. (2003) have shown that the estimates of D'_c can be affected by an error of roughly 50 %. From theoretical analyses, Tinti et al. (2004) mentioned that the difference observed in this study between the D_c values and the inferred D'_c can range between few percent up to 50 %.

For the 1999 Chi-Chi (Ji-Ji), Taiwan region, earthquake, the values of D_c inferred by Zhang et al. (2003) and Ma and Mikumo (Wang 2006a, b) can be up to 10–12 m. Although there are high uncertainties in the estimate of D_c from earthquake data (Fukuyama et al. 2003), the value of D_c from real earthquakes is much longer than that from laboratory experiments.

Several methods have been suggested to estimate D_c (Ide and Takeo 1997; Guatteri and Spudish 2000; Pulido and Irikura 2000; Ohnaka 2000; Zhang et al. 2003; Mikumo et al. 2003; Tinti et al. 2004). Those methods are essentially based on the slip history inverted from recorded seismograms. Tinti et al. (2004) clearly explained the reasons to cause the difficulty of estimating D_c. According to the correlation between D_c and η_R, Wang (2006a) proposed a method to evaluate the value of D_c from the measures of E_s and E_g. In this study, his method will be discussed in detail based on theoretical consideration and calculations from the seismic data of the 1999 M_w 7.6 Chi-Chi (Ji-Ji), Taiwan region, earthquake (see Fig. 2) which is almost a unique event specified with a complete dataset, including different types of data. In addition, some values of D_c obtained by previous studies will be reviewed.

2 Basic principle

Usually, it is not easy to estimate ΔE and E_f. Wang (2004, 2006a) suggested a way to estimate the value of ΔE, from which $E_f = \sigma_d DA$ ($D = $ slip) can be obtained from
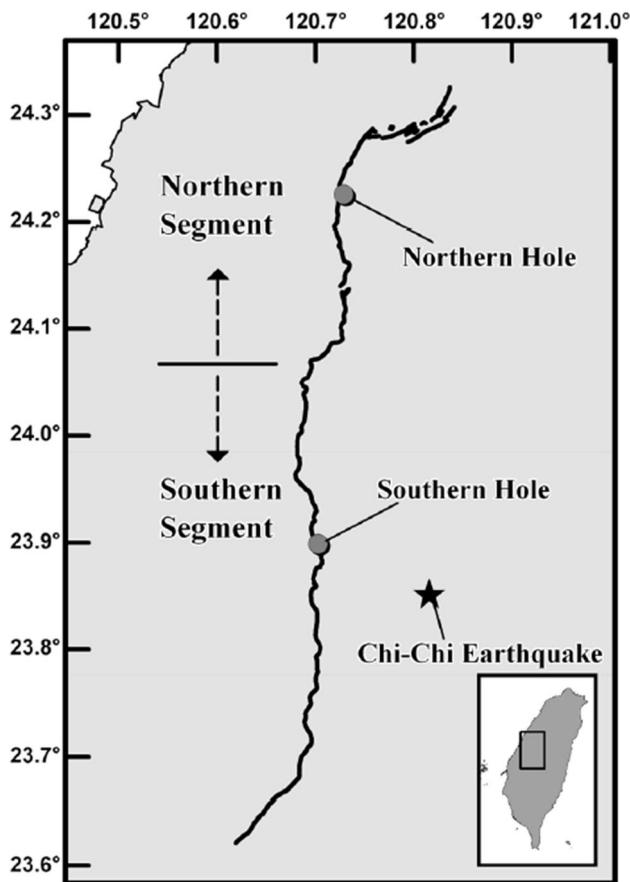
Fig. 2 A figure to show the epicenter (in a *solid star*), the Chelungpu fault (in a *line*), and the sites of two shallow boreholes (in *solid circles*) (after Wang 2006a)

$E_f = \Delta E - (E_s + E_g)$. Of course, the values of ΔE and E_f are not necessary in this study. The value of E_s can be directly measured from seismograms (cf. Wang 2004, 2006a). E_g can be evaluated indirectly from seismograms. Kanamori and Heaton (2000) suggested the following formula to evaluate the fracture energy, E_g:

$$E_g = \left[\frac{(1 - v_R/\beta)}{(1 + v_R/\beta)}\right]^{1/2} \Delta\sigma_d D_{max} A/2, \tag{1}$$

where β, v_R, $\Delta\sigma_d$, and A are, respectively, the S-wave velocity of source area, rupture velocity, dynamic stress drop, and fault area. On a simple fault plane, D_{max} is just the final displacement. On a complicated fault plane, the final displacement varies from place to place, and thus, D_{max} is the average of final displacements over the plane. Of course, the rupture velocity also varies from place to place. Equation (1) is obtained based on a crack-like rupture model (Tinti et al. 2005), and E_g computed from Eq. (1) is an average global value because $\Delta\sigma_d$ and D_{max} are both average values on the fault plane. All parameters in Eq. (1) can be evaluated from recorded seismograms and geological surveys. Define $G =$

E_g/A to be the specific fracture energy, i.e., the fracture energy per unit area. From the dislocation theory, the static-specific fracture energy is expressed by $G = \lambda K^2/Y$ (Scholz 1990), where λ is a geometry factor, K is the stress intensity factor, and Y is the Young modulus.

Based on a symmetrical circular crack model proposed by Sato and Hirasawa (1973), Ide (2002) stated that (1) E_s increases with v_R/β; (2) E_g decreases with increasing v_R/β; (3) $E_s + E_g$ increases with v_R/β; and (4) η_R increases with v_R/β, and η_R is larger than 0.6 when $v_R/\beta > 0.7$. Using a different source model, Dong and Papageorgiou (2002) also stated that η_R is an increasing function of v_R/β and larger than 0.6 when $v_R/\beta > 0.4$. Clearly, η_R approaches 1 when v_R is close to β. Faster v_R results in higher E_s. E_g is generally much smaller than ΔE, because v_R/β is usually in the range of 0.75–0.85 (Kanamori and Heaton 2000). From theoretical analyses based on friction caused by thermal pressurization, Wang (2009b) obtained a relationship between η_R and slip. The relationship suggests that η_R decreases with increasing slip and depends on model parameters of thermal pressurization.

Bizzarri (2010) theoretically explored the relationships between the fracture energy density, e.g., and the source parameters, such as the rupture velocity, v_R, the total fault slip, and the dynamic stress drop. He performed numerical simulations of three dimensional, spontaneous, fully dynamic ruptures developing on planar faults of finite width, obeying different governing laws and accounting for both homogeneous and heterogeneous friction. His results indicate that E_g depends on the adopted governing law and mainly on the rupture mode (pulse-like or crack-like, sub or supershear regime). For subshear, homogeneous ruptures, $e_g = [1 - (v_R/v_S)^2]^{1/2}$, where v_S is the shear-wave velocity, like the theoretical prediction. But for ruptures that accelerate up to supershear speeds, it is difficult to infer a clear dependence of E_g on v_R, especially in heterogeneous configurations. Hence, Eq. (1) holds only in the case of subshear events.

Venkataraman and Kanamori (2004) defined the radiation efficiency, η_R, to be the ratio of E_s to $(E_s + E_g)$. For a Model-III crack, η_R is a function of v_R/β in the following form (cf. Kanamori and Heaton 2000; Kanamori 2004; Kanamori and Brodsky 2004):

$$\eta_R = 1 - \left[\frac{(1 - v_R/\beta)}{(1 + v_R/\beta)}\right]^{1/2} \tag{2}$$

The first derivative of Eq. (2) is $d\eta_R d(v_R/\beta) = (1 - v_R/\beta)^{-1/2}(1 + v_R/\beta)^{-3/2}/2$. Since v_R/β is smaller than 1, $d\eta_R/d(v_R/\beta)$ must be positive. Obviously, there is a singularity at $v_R = \beta$. Figure 3 shows the variation of η_R with v_R/β from Eq. (2) when v_R/β ranges from 0.5 to 1.0. Clearly, η_R increases with v_R/β and the increasing rate becomes larger when $v_R/\beta > 0.90$.
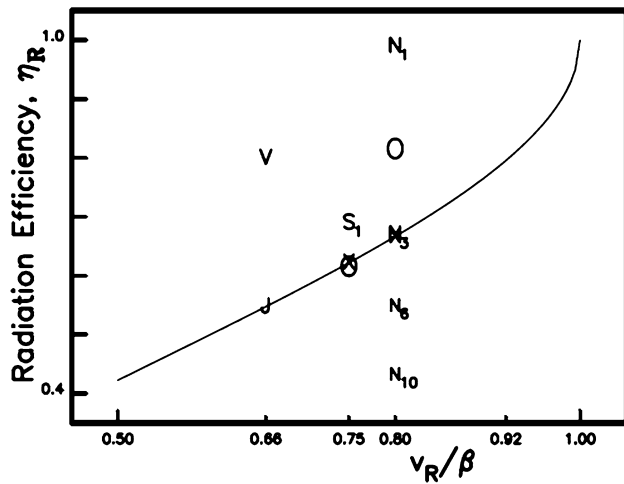
Fig. 3 The curve shows the variation of the radiation efficiency, η_R, with v_R/β calculated from Eq. (2) in the text when $v_R/\beta = 0.5-1.0$. Two crosses denote η_R at $v_R/\beta = 0.75$ and 0.80 (Ma et al. 2001). 'J' displays $\eta_R = 0.65$ at $v_R/\beta = 0.66$ by Ji et al. (2003). 'V' displays $\eta_R = 0.8$ by Venkataraman and Kanamori (2004). 'O' shows both $\eta_{RS} = 0.61$ at $v_R/\beta = 0.75$ and $\eta_{RN} = 0.81$ at $v_R/\beta = 0.80$ from Wang (2006a, b). 'S₁' denotes $\eta_{RS} = 0.69$ at $v_R/\beta = 0.75$ for $D_{cS} = 1$ m. The *symbols* 'N' with numbers represent η_{RN} at $v_R/\beta = 0.80$ when $D_{cN} = 1$, 3.7, 6, and 10 m, which are, respectively, displayed with an integer near the symbols (after Wang 2006a).

The definition of $\eta_R = E_s/(E_s + E_g)$ leads to $E_g/E_s = (1 - \eta_R)/\eta_R$. The variation in friction with slip, which is displayed by a dashed line in Fig. 1, controls the values of both E_s and E_g. The ratio E_g/E_s is also controlled by such a variation. Although E_g is a function of D_{max} from Eq. (1), D_c must be a major factor in influencing E_g because the value of E_g between D_c and D_{max} under the line CD is very small. Hence, E_g/E_s relates to D_c. In other words, D_c, which is associated with E_g/E_s, also relates to $(1 - \eta_R)/\eta_R$. hence, the value of η_R can be a constraint on the estimate of D_c.

3 Basic data for estimating D_c: an example

On September 20, 1999, the M_S 7.6 Chi-Chi (Ji-Ji), Taiwan region, earthquake ruptured the Chelungpu fault, which is a ~100-km-long and east-dipping thrust fault in central Taiwan (cf. Ma et al. 1999; Shin and Teng 2001). The epicenter and fault trace are displayed in Fig. 2. The source parameters of the earthquake were estimated by several groups of researchers from near-field and/or teleseismic seismograms with or without GPS data. The observed data and inversed results of source parameters are not uniform and vary from place to place on the fault plane. Wang (2003, 2004, 2006a, b) summarized the observed and inferred results of related source parameters from different source materials. He also pointed out the existence of

differences in source parameters between the Northern and Southern segments, which are separated almost at the middle point of the fault (see Fig. 2).

Ma and Mikumo (see Wang 2006a, b) inferred the spatial distribution of characteristic slip distance, D_c. Their values of D_c vary from 0 to 4 m, with an average of ~1 m, in the south and from 0 to 12 m, with an average of ~10 m, in the north. Ma et al. (2001) observed $v_R = 2.28$ km/s and $v_R/\beta = 0.75$ in the southern segment and $v_R = 2.69$ km/s and $v_R/\beta = 0.80$ in the northern one. Huang et al. (2001) evaluated the values of $\Delta\sigma_s$ for the two segments from near-field seismograms. Hwang et al. (2001) measured the values of E_s from near-fault seismograms. Wang (2004) correlated their values by eliminating the effect due to finite frequency bandwidth limitation. The correlated results are $E_{sN} = 3.981 \times 10^{16}$ J for the northern segment, $E_{sS} = 0.326 \times 10^{16}$ J for the southern one, and $E_s = E_{sS} + E_{sN} = 4.307 \times 10^{16}$ J for the whole fault.

In order to calculate the values of E_g for the 1999 Chi-Chi earthquake from Eq. (1), the basic values of parameters in use (Wang 2006a, b) are (1) $v_{RS} = 0.75\beta$, $\Delta\sigma_{dS} = 6.52$ MPa, $D_{cS} = 1$m, and $A_S = 4.551 \times 10^8$ m² for the southern segment; and (2) $v_{RN} = 0.80\beta$, $\Delta\sigma_{dN} = 2.97$ MPa, $D_{cN} = 10$ m, and $A_N = 3.615 \times 10^8$ m² for the northern one. The estimated values of G and E_g are (1) for the southern segment, $G_S = 9.32 \times 10^5$ J/m² and $E_{gS} = 4.24 \times 10^{14}$ J, which is 13 % of E_{sS}; (2) for the northern segment, $G_N = 3.68 \times 10^7$ J/m² and $E_{gN} = 1.33 \times 10^{16}$ J, which is 33 % of E_{sN}; and (3) for the whole fault, $G = 1.68 \times 10^7$ J/m² and $E_g = E_{gS} + E_{gN} = 1.37 \times 10^{15}$ J, which is 32 % of E_s. The values of η_R are 0.88 for the Southern segment, 0.75 for the Northern one, and 0.76 for the whole fault. Based on the inverted results of source rupture processes from teleseismic data, Ma and Mikumo (see Wang 2006a, b) obtained $G = (1-3) \times 10^8$ J/m², with the largest value in the grid having the greatest displacement. Their values are about one-order-of-magnitude larger than those by Wang (2006a, b). The difference might be due to the use of different kinds of data by respective studies. They also observed an increase in G from south to north. Venkataraman and Kanamori (2004) evaluated the radiation efficiency of $\eta_R = 0.8$ for the earthquake from teleseismic data, thus giving $E_g \approx 0.25 E_s$. Obviously, the value of E_g measured from near-fault seismograms is similar to that from teleseismic data. Hence, the results are reliable. The data to be used in this study, i.e., E_s, D (average displacement), D_c, E_g, η_R, and G, are given in Table 1. In the table, E_g is evaluated through two ways: (1) from Eq. (1) with $D_S = 4.88$ m and $D_N = 7.15$ m; and (2) from Eq. (3) as mentioned below with $D_{cS} = 1$ m and $D_{cN} = 1$, 3.7, 6, and 10 m. Meanwhile, in the table, the subscripts "S" and "N"

Table 1 Related values in use

Segment	D (m)	D_c (m)	E_s (10^{16} J)	E_g (10^{16} J)	η_R	G (10^7 J/m^2)	Way of evaluation
S	4.88	1.4	0.33	0.21	0.61	0.45	(1)
		1.0	0.33	0.15	0.69	0.33	(2)
N	7.15	1.8	3.98	0.95	0.81	2.59	(1)
		1.0	3.98	0.54	0.99	1.44	(2)
		3.7	3.98	1.99	0.67	5.34	(2)
		6.0	3.98	3.22	0.55	8.64	(2)
		10.0	3.98	5.37	0.43	14.4	(2)

E_s evaluated by Wang (2004); D (the average value over a fault segment), D_c, E_g, η_R, and G evaluated by Wang (2006a), E_g is evaluated through two ways: (1) from Eq. (1) with $D_{maxS} = 4.88$ m and $D_{maxN} = 7.15$ m; and (2) from Eq. (2) with $D_{cS} = 1$ m and $D_{cN} = 1, 3.7, 6$, and 10 m. (Subscripts: "S" and "N" for the southern and northern segments of the Chelungpu fault, respectively)

are, respectively, applied to show the southern and northern segments of the Chelungpu fault.

In 2000, two shallow boreholes near the Chelungpu fault (see Fig. 2) were drilled under a Taiwan-Japan Collaborative Project (cf. Tanaka et al. 2002). The possible fracture zones associated with the Chi-Chi (Ji-Ji) earthquake are in the range of 225–330 m at the northern borehole and 177–180 m at the southern one. Different depths of the inferred fracture zones are mainly due to the difference in the distances of the boreholes to the fault trace. The values of related physical parameters obtained from the two holes can be seen in Wang (2010). From the core samples, Otsuki et al. (2001) and Tanikawa et al. (2004) obtained $D_c = {\sim}1$ m at the northern borehole. This value of D_c is close to the average of D_c in the southern segment inferred by Ma and Mikumo (See Wang 2006a, b) from teleseismic data and much shorter than those inferred by Zhang et al. (2003) and Ma and Mikumo (see Wang 2006a, b) for the northern segment from teleseismic data.

4 Estimates of D_c and discussion

Numerous factors can influence D_c. From laboratory experiments, Wong (1982) found that temperature, pressure, rock type etc., can all change the shear fracture energy up to an order of magnitude. Marone (1998) observed that these factors are also able to influence the value of D_c. Kostrov and Das (1988) obtained $G = 1 - 10^2$ J/m^2 for a single crystal. Scholz (1990) reported $G = 0.27 - 10^2$ J/m^2 for some geological materials and $G = 10^6 - 10^7$ J/m^2 for earthquakes. In addition, $G = 1.1 \times 10^3$ J/m^2 when the materials melt and $G = 1.1 \times 10^5$ J/m^2 in the condition of dissociation. Pittarello et al. (2008) estimated the surface energy from microcrack density inside clast (i.e., cracked grains) entrapped in the pseudotachylyte and in the fault wall rock and the values

range between 0.10 and 0.85×10^3 J/m^2. Their estimates for the studied fault segments suggest that ${\sim}97\,\%$–99 % of the energy was dissipated as heat during seismic slip. They concluded that at 10 km depth, less than 3 % of the total mechanical work density is adsorbed as surface energy on the fault plane during earthquake rupture.

The theoretical values of G are usually calculated for a homogeneous model, with constant K and Y, under a normal temperature and a constant pressure. Whereas the temperature, lithostatic pressure, and rock properties on the fault plane change with depth, and, thus, K and Y must also be a function of depth. This suggests depth-dependence of G. Of course, these properties also vary from place to place, and, thus, K and Y must also be a function of locality. The observation of $G_N > G_S$ by Ma and Mikumo (see Wang 2006a, b) as mentioned above indicates the differences on the temperature, lithostatic pressure, and rock properties between the southern and northern fault segments. Huang and Wang (2002) observed the changes of scaling of displacement spectra of the 1999 Chi-Chi (Ji-Ji), Taiwan region, earthquake from near-fault seismograms from south to north. From the observed and inferred results, Wang (2003, 2004, 2006a, b) pointed out the differences in source parameters between the northern and southern segments. Wang (2006a) found the difference of pore pressures between the two fault segments. From seismic reflection experiments, Wang et al. (2004) also observed a difference in sub-surface fault geometry between the two segments. Consequently, different physical properties between the northern and southern segments lead to $G_N > G_S$. Bizzarri (2011) stressed that a large number of chemical and physical mechanisms can also affect D_c.

Since the measured value of D_c is usually in the range of 0.1 m to few meters from earthquake data (Mikumo et al. 2003), the value of $D_{cS} = 1$ m for the southern fault segment inferred by Zhang et al. (2003) and Ma and Mikumo

(see Wang 2006a, b) is reasonable. On the other hand, their values of $D_{cN} = \sim 10$ m for the northern fault segment sound to be unusual, even though it is less than the maximum displacement of 15 m at the depth of 8 km on the northern fault plane as inferred by Ma et al. (2001). There are two possible reasons for causing large D_{cN}. The first one is an under-shot of the northern segment during faulting, thus resulting in a fact that D_{cN} was almost the final offset. This does not seem possible, because there was a long slip displacement of 15 m on the fault plane as mentioned above. The second reason is that the value of $D_{cN} = 10$ m was over-estimated, thus resulting in an over-estimate of E_{gN}. The second reason seems reasonable. However, it is actually difficult to ensure an exact value of D_c based on the inferred stress-slip function from seismograms as pointed out by Tinti et al. (2004). Fukuyama et al. (2001) stressed that there is high uncertainty in the estimate of D_c. Here, it is necessary to explore the acceptable range of D_c for the Northern segment.

Equation (2) shows that the ratio of the rupture velocity to shear-wave velocity, i.e., v_R/β, is the main parameter causing an overall effect on η_R. Hence, the effect on η_R due to this ratio must be considered in advance. In the following, the value of η_R calculated from Eq. (2) is denoted by η_{RC}. Ma et al. (2001) observed $v_R/\beta = 0.75$ in the southern segment and $v_R/\beta = 0.80$ in the northern one. The related values of η_R calculated from Eq. (2) are $\eta_{RCS} = 0.62$ at $v_R/\beta = 0.75$ for the southern segment and $\eta_{RCN} = 0.67$ at $v_R/\beta = 0.80$ for the northern one, and the data points are denoted by two crosses in Fig. 3. Based on Eq. (1), Venkataraman and Kanamori (2004) evaluated the value of E_g from $v_R/\beta = 0.66$ by Ji et al. (2003), and the values of $\Delta\sigma_d$, D_{max}, and A by Ma et al. (2001). Hence, their value of η_R is 0.8. The related data point is denoted by 'V' in Fig. 3. For $\eta_R = 0.8$, from Eq. (2), the related value of v_R/β is 0.92 which is larger than 0.66 inferred by Ji et al. (2003). On the other hand, the value of η_{RC} calculated from $v_R/\beta = 0.66$ inferred by Ji et al. (2003) based on Eq. (2) is 0.55 and is shown by a symbol 'J' in Fig. 3. Since $v_R/\beta = 0.66$ by Ji et al. (2003) is the smallest in comparison with those inferred by others, $\eta_R = 0.55$ must be the smallest one based on the increase in η_R with v_R/β as displayed in Fig. 3. Clearly, the value of $\eta_R = 0.8$ is larger than $\eta_R = 0.55$. For the southern segment, the measured and calculated values are, respectively, $\eta_{RS} = 0.61$ (displayed by a symbol 'O' in Fig. 3) and $\eta_{RCS} = 0.62$. The two values are similar to each other. For the northern segment, the two values are, respectively, $\eta_{RN} = 0.81$ (demonstrated also by a symbol 'O' related to $v_R/\beta = 0.80$ in Fig. 3) and $\eta_{RCN} = 0.66$. The former is 0.14 larger than the latter. This inconsistency might be due to either an over-estimate of E_s or an under-estimate of η_R using Eq. (2). Since Wang (2004) eliminated possible effects on the estimate of E_s due

to several factors, including the finite frequency bandwidth limitation, site effect, path effect, and radiation pattern, so his measured values should be reliable. Hence, it is assumed that this inconsistency is due to an under-estimate of η_R using Eq. (2), which was obtained based on dry rocks. Indeed the mechanisms due to fluids, for example, lubrication (Brodsky and Kanamori 2001) or thermal fluid pressurization (Sibson 1973; Mase and Smith 1984/1985), also play a significant role on faulting. Since the ratio v_R/β in Eq. (2) cannot represent such mechanisms, an advanced model including such mechanisms is needed to construct.

Since D_c is usually in the range of 0.1 m to few meters from earthquake data (Ide and Takeo 1997; Mikumo et al. 2003), the maximum values of D_{cN}, i.e., 10 and 12 m, and the average ones, i.e., 6 and 10 m, inferred, respectively, by Zhang et al. (2003) and Ma and Mikumo (see Wang 2006a, b) seem to be unusually large. In principle, at any locality on the fault plane, D_{max} must be larger than D_c, and, thus, on the whole fault plane average, D_{max} should be also larger than average D_c. The average value of D_c (= 10 m) inferred by Ma and Mikumo (see Wang 2006a, b) is larger than the average displacement $D_N = 7.15$ m, even though it is smaller than $D_{maxN} = 15$ m at $H = 8$ km inferred by Ma et al. (2001). Scholz (1988) stressed that the fault would be stable and could not generate large earthquakes if D_c is too long. This means that D_c cannot be larger than average D_N. Hence, $D_{cN} = 10$ m was over-estimated. Of course, $D_{cN} = 6$ m could also be over-estimated, even though it is smaller than the average $D_N = 7.15$ m. Fukuyama et al. (2003) stressed that there is high uncertainty in estimates of D_c from the inferred stress-slip function. Hence, it is necessary to explore the range of D_{cN}.

Wang (2006a) proposed a way to explore the acceptable value or range of D_c. The way is discussed in detail here. From Fig. 1, E_g can be approximated by

$$E_g \approx \frac{\Delta\sigma_d D_c A}{2}. \tag{3}$$

It is noted that since the variation of stress versus slip must be described by the dashed line in Fig. 1, Eq. (3), of course, gives an approximation and upper bound estimate of E_g. E_g estimated from Eq. (3) is slightly smaller than that done from Eq. (1). The difference between the values of E_g evaluated from the two equations depends on the stress drops, frictional strengths, frictional law, and the nonlinear decrease of stress with increasing slip. From Eq. (3), we can calculate the value of η_R from $E_s/(E_s + E_g)$, where E_s was taken from Wang (2004). A comparison between Eqs. (1) and (3) suggests an approximated relation of D_c versus D_{max}:

$$D_c \approx \left[\frac{(1 - v_R/\beta)}{(1 + v_R/\beta)}\right]^{1/2} D_{max}. \tag{4}$$

It is noted that Eq. (4) does not hold for supershear earthquakes. Like E_g, D_c estimated from Eq. (4) is slightly different than that obtained from the inferred stress-slip function. Nevertheless, Eq. (4) is still acceptable because only the comparison of the values of η_R calculated from several values of D_c is taken into account.

Based on Eq. (3), $D_{cS} = 1$ m gives $E_{gS} = 0.15 \times 10^{16}$ J and thus $\eta_{RS} = 0.69$, which is only slightly larger $\eta_{RCS} = 0.62$ as mentioned above and represented by 'S$_1$' in Fig. 3 for the southern segment. From Eq. (4), we have $D_{cS} = 1.4$ m from $D_{maxS} = 4.88$ m inferred by Ma and Mikumo (see Wang 2006a, b). The two values of D_{cS} are close to each other, thus suggesting that $D_{cS} = 1$ m is acceptable.

In order to explore the acceptable values of D_{cN} for the northern segment, η_{RN} is calculated for five particular values of D_{cN} when $\Delta\sigma_d = 2.97$ MPa and $v_R/\beta = 0.80$. For the first case, we take the value of $D_{cN} = 1.8$ m calculated from the average displacement on the northern fault plane of average $D_{maxN} = 7.15$ m inferred from seismograms (cf. Wang 2006b) based on Eq. (4). This leads to $\eta_{RN} = 0.81$. Its data point is the same as that denoted by 'O' related to $v_R/\beta = 0.80$ in Fig. 3. For the second case 2, we take $D_{cN} = 1$ m inferred by Tanikawa et al. (2004) from the core samples obtained at the depth range of 225–330 m in a shallow northern borehole by using numerical simulations based on the thermal pressurization model. This leads to $E_{gN} = 0.54 \times 10^{16}$ J and $\eta_{RN} = 0.99$, which is represented by 'N$_1$' in Fig. 3. For the third case, considering $E_{sN} = 3.98 \times 10^{16}$ J with $\Delta\sigma_{dN} = 2.97 \times 10^7$ N/m^2 and $A_N = 3.929 \times 10^8$ m^2 measured from seismograms (Wang 2004, 2006a), we have $D_{cN} = 3.7$ m. This gives $\eta_{RN} = 0.67$ at $v_R/\beta = 0.80$. Its data point is denoted by a symbol 'N$_3$'. For the fourth case, considering $D_{cN} = 6$ m, which was inferred by Zhang et al. (2003), we have $E_{gN} = 3.22 \times 10^{16}$ J. This leads to $\eta_{RN} = 0.55$, and the related data point is shown by 'N$_6$' in Fig. 3. For the fifth case, considering $D_{cN} = 10$ m, which was inferred by Ma and Mikumo (see Wang 2006a, b), we have $E_{gN} = 5.37 \times 10^{17}$ J. This leads to $\eta_{RN} = 0.43$, and the related data point is shown by 'N$_{10}$' in Fig. 3. Obviously, η_{RN} decreases with increasing D_{cN}. Related values of E_{sN}, E_{gN}, G_N, and η_{RN} of the five cases are listed in Table 1.

Since the value of $D_{cN} = 1$ m was inferred by Tanikawa et al. (2004) from the core samples at a shallow borehole, it can only represent the value of D_{cN} at shallow depths and thus cannot be the average of D_{cN} over the northern segment. The value of $D_{cN} = 1.8$ could be the lower bound of D_{cN}, because it was calculated from the average $D_{maxN} = 7.15$ m inferred from seismograms and larger than 1 m for the shallow depths. The data point denoted by 'N$_3$' related to $D_{cN} = 3.7$ m calculated from

$E_{sN} = 3.98 \times 10^{16}$ J with $\Delta\sigma_{dN} = 2.97 \times 10^7$ N/m^2 and $A_N = 3.929 \times 10^8$ m^2 measured from seismograms is much close to the data point denoted by a cross on the theoretical curve in Fig. 3. Hence this $D_{cN} = 3.7$ m could be the upper bound of D_{cN}. The two values of the fourth and fifth cases are both smaller than those (0.75–0.95) of normal earthquakes (Kanamori and Brodsky 2004), and their data points are below the theoretical curve. Hence, $D_{cN} = 6$ and 10 m could be over-estimated. In addition, $\eta_{RN} = 0.81$ of case 2 and 0.67 of case 3, respectively, related to $D_{cN} = 1.8$ and 3.7 m are both larger than $\eta_{RS} = 0.61$. Hence, it is reasonable to consider D_{cN} to be in between 1.8 and 3.7 m. The mean value of the two values is 2.25 m, which is close to $D_{cN} = 2.3$ m inferred by Mori (2005) from near-fault seismograms. Conclusively, the acceptable value of D_{cN} must be in between 1.8 and 3.7 m, with the mean value of 2.25 m to be most acceptable one.

5 Conclusions

The characteristic slip displacement (or slip-weakening distance), D_c, of the velocity- and state-dependent friction law is an important parameter of friction law and its value varies in a large range. Meanwhile, the values measured from laboratory experiments are much smaller than those estimated from seismic data. Essentially, it is difficult to estimate an acceptable value of D_c. Nevertheless, seismologists need its value to understand the source processes. In this study, a simple way is proposed to estimate D_c based on the constraint from the radiation efficiency, i.e., $\eta_R = E_s/(E_s + E_g)$. In order to describe the way clearly, an example of estimate of D_c is made for the 1999 M_w 7.6 Chi-Chi (Ji-Ji) earthquake, which ruptured along the Chelungpu fault in central Taiwan region, because there are fruitful data generated by this event. The values of D_c for the two segments of the fault were estimated by Zhang et al. (2003) and Ma and Mikumo (see Wang 2006a, b). Results are, respectively, $D_{cS} = 1$ m (for the southern segment) and $D_{cN} = 10$ m (for the northern segment). D_{cS} seems to be reasonable, while D_{cN} is too long to fit the theoretical requirement. From the measured and calculated values of η_R for five values of D_{cN} through two approaches, the acceptable value of D_{cN} is in between 1.8 and 3.7 m. The mean value of 2.25 m is considered to be the most acceptable one.

References

Beeler NM, Tullis TE, Weeks JD (1994) The roles of time and displacement in the evolution effect in rock friction. Geophys Res Lett 21:1987–1990

Bizzarri A (2010) On the relations between fracture energy and physical observables in dynamic earthquake models. J Geophys Res 115(B10307):2009J. doi:10.1029/B007027

Bizzarri A (2011) On the deterministic description of earthquakes. Rev Geophys. doi:10.1029/2011RG000356

Brodsky EE, Kanamori H (2001) Elastohydrodynamic lubrication of faults. J Geophys Res 106:16357–16374

Dieterich JH (1978) Time-dependent friction and the mechanics of stick-slip. Pure Appl Geophys 116:790–806

Dieterich JH (1979) Modeling of rock friction 1. Experimental results and constitutive equations. J Geophys Res 84:2161–2168

Dieterich JH (1992) Earthquake nucleation on faults with rate- and state-dependent strength. Tectonophysics 211:115–134

Dong G, Papageorgiou AS (2002) Seismic radiation from unidirectional asymmetrical circular crack model. Bull Seismol Soc Am 92(3):945–961

Fukuyama E, Mikumo T, Olsen KB (2003) Estimation of the critical slip-weakening distance: theoretical background. Bull Seismol Soc Am 93(4):1835–1840

Gu JC, Rice R, Ruina AL, Tse ST (1984) Slip motion and stability of a single degree of freedom elastic system with rate and state dependent friction. J Mech Phys Solids 32:167–196

Guatteri M, Spudich P (2000) What can strong-motion data tell us about slip-weaken fault-friction laws? Bull Seismol Soc Am 90:98–116

Huang MW, Wang JH (2002) Scaling of displacement spectra of the 1999 Chi-Chi, Taiwan, earthquake from near-fault seismograms. Geophys Res Lett 29(27):1–4

Huang WG, Wang JH, Huang BS, Chen KC, Chang TM, Hwang RD, Chiu HC, Tsai CC (2001) Estimates of source parameters for the Chi-Chi, Taiwan, earthquake, based on Brune's source model. Bull Seismol Soc Am 91:1190–1198

Hwang RD, Wang JH, Huang BS Chen, Huang WG, Chang TM, Huang RD, Chiu HC, Tsai CC (2001) Estimates of stress drop from near-field seismograms of the M_S 7.6 Chi-Chi, Taiwan, earthquake of September 20, 1999. Bull Seismol Soc Am 91:1158–1166

Ide S (2002) Estimation of radiated energy of finite-source earthquake models. Bull Seismol Soc Am 92:2994–3005

Ide S, Takeo M (1997) Determination of constitutive relations of fault slip based on seismic wave analysis. J Geophys Res 102:27379–27391

Ji C, Helmburger D, Wald DJ, Ma KF (2003) Slip history and dynamic implications of the 1999 Chi-Chi, Taiwan, earthquake. J Geophys Res 108(B9):2412. doi:10.1029/2002JB001764

Kanamori H (2004) The diversity of the physics of earthquakes. Proc Jpn Acad 80:297–316

Kanamori H, Brodsky EE (2004) The physics of earthquakes. Rep Prog Phys 67:1429–1496

Kanamori H, Heaton TH (2000) Microscopic and macroscopic physics of earthquakes. In: Rundle JB, Turcotte DL, Klein W (eds) Geocomplexity and Physics of Earthquakes, Geophysical Monograph 120 AGU, Washington DC, pp 147–163

Kostrov BV, Das S (1988) Principles of earthquake source dynamics. Cambridge University Press, Cambridge, pp 1–286

Ma KF, Lee CT, Tsai YB, Shin TC, Mori J (1999) The Chi-Chi, Taiwan earthquake: large surface displacements on an inland thrust fault. EOS Trans AGU 80:605–611

Ma KF, Mori J, Lee SJ, Yu SB (2001) Spatial and temporal distribution of slip for the 1999, Chi-Chi, Taiwan, earthquake. Bull Seismol Soc Am 91:1069–1087

Marone C (1998) Laboratory-derived friction laws and their application to seismic faulting. Annu Rev Earth Planet Sci 26:643–669

Mase CW, Smith L (1984/1985) Pore-fluid pressures and frictional heating on a fault surface. Pure Appl Geophys 122:583–607

Mikumo T, Fukuyama E, Olsen KB, Yagi Y (2003) Stress-breakdown time and slip-weakening distance inferred from slip-velocity functions on earthquake faults. Bull Seismol Soc Am 93(1):264–282

Mori J (2005) Using near-field seismograms to estimate the slip weakening distance. Eos Trans AGU Suppl 86(52):F1420

Ohnaka M (2000) A physical scaling relation between the size of an earthquake and its nucleation zone size. Pure appl Geophys 157:2259–2282

Otsuki K, Uzuki T, Koizumi Y (2001) Presentation on core analysis, In: Proceedings of ICDP workshop on drilling the Chelungpu Fault, Taiwan, Taipei, p 37

Pittarello L, Di Toro G, Bizzarri A, Pennacchioni G, Hadizadeh Cocco M (2008) Energy partitioning during seismic slip in pseudotachylyte-bearing faults (Gole Larghe Fault, Adamello, Italy). Earth Planet Sci Lett 269:131–139. doi:10.1016/j.epsl.2008.01.052

Pulido N, Irikura K (2000) Estimation of dynamic rupture parameters from the radiated seismic energy and apparent stress. Geophys Res Lett 27:3945–3948

Reinen LA, Weeks JD (1993) Determination of rock friction constitutive parameters using an iterative least-squares inversion method. J Geophys Res 98:15937–15950

Rice JR (1983) Constitutive relations for fault slip and earthquake instabilities. Pure appl Geophys 121:443–475

Rice JR, Ben-Zion Y (1996) Slip complexity in earthquake fault models. Proc Natl Acad Sci USA 93:3811–3818

Rice JR, Ruina AL (1983) Stability of steady frictional slipping. J Appl Mech 50:343–349

Rice JR, Tse ST (1986) Dynamic motion of a single degree of freedom system following rate and state dependent friction law. J Geophys Res 91:521–530

Roy M, Marone C (1996) Earthquake nucleation on model faults with rate- and state-dependent friction: effects of inertia. J Geophys Res 101:13919–13932

Ruina A (1983) Slip instability and state variable friction laws. J Geophys Res 88:10359–10370

Sato T, Hirasawa T (1973) Body wave spectra from propagating shear crack. J Phys Earth 21:415–431

Scholz GH (1988) The critical slip distance from seismic faulting. Nature 336:761–763

Scholz GH (1990) The mechanics of earthquakes and faulting. Cambridge University Press, Cambridge

Shin TC, Teng TL (2001) An overview of the 1999 Chi-Chi, Taiwan, earthquake. Bull Seismol Soc Am 91:895–913

Sibson RH (1973) Interactions between temperature and pore fluid pressure during earthquake faulting—a mechanism for partial or total stress relief. Nat Phys Sci 243:66–68

Tanaka H, Wang CY, Chen WM, Sakaguchi A, Ujiie K, Ando M (2002) Initial science report of shallow drilling penetrating into the Chelungpu fault zone, Taiwan. Terr Atmos Ocean Sci 13(3):227–251

Tanikawa W, Noda H, Mizoguchi K, Shimamoto T, Hung JH (2004) Frictional and hydraulic properties of the Chelungpu fault zone and their implications for rupture propagation during the 1999 Chi-Chi earthquake, In: Abstract Vol 1, Joint AOGS 1st annual meeting & 2nd APHW conference, July 5–9, Singapore, pp 43–44

Tinti E, Bizzarri A, Piatanesi A, Cocco M (2004) Estimates of slip weakening distance for different dynamic rupture models. Geophys Res Lett 31:L02611. doi:10.1029/2003GL018811

Tinti E, Spudich P, Cocco M (2005) Earthquake fracture energy inferred from kinematic rupture models on extended faults. J Geophys Res 110:B12303. doi:10.1029/2005JB003644

Ulutaş E (2008) Site corrections for strong ground motion stations by using peak ground accelerations in Marmara region, NW Turkey. EGU General Assembly, Vienna, Austria, 13–18 April 2008, Geophysical Research Abstracts, Vol 10, EGU2008-A-00488

Ulutaş E (2013) Comparison of the seafloor displacement from uniform and non-uniform slip models on tsunami simulation of the 2011 Tohoku-Oki earthquake. J Asian Earth Sci 62:568–585. doi:10.1016/j.jseaes.2012.11.007

Ulutaş E (2015) An innovative approach for seismic zonation by using geographical information system. In: 3th international symposium on innovative technologies in engineering and science, 3–5 June 2015, Valencia

Ulutaş E, Aşçı M, Çetinol T, Yas T, Güven İT, Barış Ş, Özer MF (2006) Liquefaction hazard of İzmit urban area by using geographic information system. In: 17th international geophysical congress and exhibition, Nov 14–17, Ankara

Ulutaş E, Coruk Ö, Karakaş A (2011) A study of residuals for strong ground motions in Adapazarı Basin, NW Turkey, by ground motion prediction equations (GMPEs). Stud Geophys Geod 55:213–240

Venkataraman A, Kanamori H (2004) Observational constraints on the fracture energy of subduction zone earthquakes. J Geophys Res 109(B05302):1–20

Wang JH (2002) A dynamical study of two one-state-variable, rate-dependent and state-dependent friction laws. Bull Seismol Soc Am 92:687–694

Wang JH (2003) A one-body dynamic model of the 1999 Chi-Chi, Taiwan, earthquake. Terr Atmos Ocean Sci 14(3):335–342

Wang JH (2004) The seismic efficiency of the 1999 Chi-Chi, Taiwan, earthquake. Geophys Res Lett 31:L10613. doi:10.1029/204GL0194172004

Wang JH (2006a) Energy release and heat generation during the 1999 Chi-Chi, Taiwan, earthquake. J Geophys Res 111:B11312. doi:10.1029/2005JB004018

Wang JH (2006b) A review of the source parameters of the 1999 Chi-Chi, Taiwan, earthquake. Terr Atmos Ocean Sci 17:179–202

Wang JH (2009a) A numerical study of comparison between two one-state-variable, rate- and state-dependent friction evolution laws. Earthq Sci 22:197–204

Wang JH (2009b) Effect of thermal pressurization on the radiation efficiency. Bull Seismol Soc Am 99:2293–2304

Wang JH (2010) Summary of physical parameters measured at several boreholes cutting the Chelungpu fault in central Taiwan. Terr Atmos Ocean Sci 21:655–673

Wang CY, Li CL, Lee HC (2004) Constructing subsurface structures of the Chelungpu fault to investigate mechanisms leading to abnormally large ruptures during the 1999 Chi-Chi earthquake, Taiwan. Geophys Res Lett 31:L02608. doi:10.1029/L018323

Wong TF (1982) Shear fracture energy of Westerly granite from post-failure behavior. J Geophys Res 87(B2):990–1000

Zhang W, Iwata T, Irikura K, Sekiguchi H, Bouchon M (2003) Heterogeneous distribution of the dynamic source parameters of the 1999 Chi-Chi Taiwan, earthquake. J Geophy Res 108:B5. doi:10.1029/2002JB001889